

The Effect of Osmotically Induced Water Flows on the Permeability and Ultrastructure of the Rabbit Gallbladder

Anthony P. Smulders, John McD. Tormey,
and Ernest M. Wright

Department of Physiology, University of California Medical Center,
Los Angeles, California 90024

Received 28 June 1971

Summary. The purpose of these experiments was to determine the effect of osmotic gradients on the permeability of the rabbit gallbladder. Increasing the tonicity of the mucosal solution reduced the permeability of the gallbladder to both ions and non-electrolytes, whereas there was no significant effect when the serosal solution was made hypertonic. These results cannot be explained by solvent/solute interactions in either the epithelial membranes or the unstirred layers. Associated with the changes in permeability was the appearance of the transport number effect and current induced resistance changes. Morphological studies of the gallbladder under these conditions showed that the extracellular spaces of the epithelium and the rest of the wall dilate in the presence of osmotic flow to the serosa, but that the spaces collapse when the flow is in the opposite direction. Reconstruction of the permeability changes from the dimensions of the tissue show that all the physiological phenomena are accounted for by the changes in morphology, the dominant effect being in the lateral intercellular spaces. These results suggest that the lateral spaces are a common pathway shared by all solutes crossing the epithelium, and that diffusion along these spaces becomes rate limiting as the spaces collapse.

Over the last decade an ever increasing amount of attention has been focused on the role of the lateral intercellular spaces in the transport of solutes and water across epithelial membranes. This has been especially true since the reports that these spaces widely dilate during isotonic water transport across the rabbit gallbladder (Diamond & Tormey, 1966; Kaye, Wheeler, Whitlock & Lane, 1966; Tormey & Diamond, 1967). The purpose of the present two papers is to describe experiments which demonstrate the importance of the lateral channels in the passive movement of solutes and

water across the rabbit gallbladder. The first paper describes the effects of osmotic gradients on passive unidirectional fluxes of nonelectrolytes, electrical conductance and the ultrastructure of the tissue, whereas the second paper (Wright, Smulders & Tormey, 1972, hereafter referred to as Paper 2) describes the effects on water permeability. Our results suggest that the lateral intercellular spaces are a common pathway shared by all solutes crossing the epithelium, and that diffusion along the spaces is rate limiting under certain circumstances. Preliminary accounts of some of this work have already been presented (Tormey, Smulders & Wright, 1971; Tormey, Wright & Smulders, 1971).

Materials and Methods

The object of these experiments was to generate osmotic flows across the rabbit gallbladder and measure the effect of these flows on unidirectional nonelectrolyte fluxes, tissue resistance and anatomical structure.

Gallbladders were removed from male white rabbits, rinsed free of bile, cut open along the mesenteric border, and mounted as flat sheets between two lucite half-chambers. The area of the window between the half-chambers was 1.13 cm^2 and each reservoir contained 10 ml of physiological saline which was recirculated by means of an oxygen gas lift. For further details *see* Smulders and Wright (1971).

All experiments were carried out at room temperature (22 to 24 °C) in saline which contained NaCl (0.148 M), KCl (0.006 M) and CaCl_2 (0.00025 M), buffered at pH 7.4 with $\text{Na}_2\text{HPO}_4/\text{NaH}_2\text{PO}_4$ (0.0025 M). Nonelectrolytes were added to this solution to give final concentrations which ranged from 0.01 to 0.6 M. The ^{14}C labeled isotopes were obtained from the New England Nuclear (Boston, Mass.) and International Chemical and Nuclear (Irvine, Calif.) Corporations. Statistical errors are quoted as the standard error of the mean with the number of estimates in parentheses. Physiological parameters are expressed in terms of the serosal area of the gallbladder, i.e., the area of the window between the half-chambers, except in Table 3 where they are expressed in terms of the mucosal area.

Electrical Measurements

The electrical potential difference (p.d.) across the gallbladder was measured on a Keithley electrometer, Model 610B, and recorded on a Varian potentiometric chart recorder, G11A. The electrometer was connected to the mucosal and serosal solutions via calomel half-cells and agar salt bridges.

The resistance of the gallbladder was measured by recording the change in p.d. within 2 sec of passing a direct current (100 μamp) across the tissue. The resistance values were corrected for the resistance of the solution between the tips of the salt bridges used to monitor the p.d.

Flux Measurements

Nonelectrolyte fluxes across the gallbladder were determined by the use of radioactive tracer techniques. Briefly, a tracer quantity of a ^{14}C labeled compound was added to the solution on either the mucosal or serosal side of the tissue and the rate of appearance

of the isotope in the solution on the opposite side was measured by withdrawing aliquots of the 'cold' solution at 15-min intervals. The radioactive samples were then assayed by conventional liquid scintillation counting techniques where each sample was counted to a standard error of 1% or less. Fluxes are expressed in $\mu\text{moles}/\text{cm}^2/\text{hr}$. Previous experiments have shown that steady-state nonelectrolyte fluxes are obtained within 15 min and that the fluxes remain constant for at least 8 hr (Smulders & Wright, 1971).

Anatomical Methods

Experiments in which gallbladders were destined for anatomical study were carried out between a pair of slightly modified chambers. The gallbladders were held sandwiched between two thin plastic gaskets. Without disturbing the geometry of the tissue, the gaskets, with the gallbladder between them, could be removed from the chamber and dropped into the fixative in less than 2 sec. The two faces of the gallbladder remained in contact with their respective bathing solutions until the actual moment of contact with the fixative. Although most gallbladders were fixed by direct immersion, we were concerned that during the time between dropping the tissue into fixative and the actual fixation of structure, changes in the tissue geometry produced by osmotic gradients might significantly reverse. Accordingly, a few gallbladders were fixed *in situ* between the half-chambers; the mucosal and serosal solutions were replaced by saline solutions containing in addition either 1% glutaraldehyde or 1% osmium tetroxide. Results were similar to those obtained by simple immersion fixation.

We were particularly concerned that the fixatives themselves might set up osmotic water flow. Addition of glutaraldehyde to the mucosal solution generated a streaming potential and produced no change in tissue resistance for at least 2 hr. The glutaraldehyde reflection coefficient was estimated to be about 0.7 from the magnitude of the streaming potentials (*see* Wright & Diamond, 1969*a*). The glutaraldehyde is thus capable of producing an osmotic flow across the epithelium which could possibly alter the fine structure of the tissue (*cf.* Grantham, Cuppage & Fanestil, 1971). Simultaneous addition of glutaraldehyde to both the mucosal and serosal solutions does not completely eliminate this problem since the much larger serosal unstirred layer retards the diffusion of substances up to the serosal face of the epithelium; i.e., there are transient local osmotic gradients across the tissue. This effect became apparent when we attempted to fix gallbladders in the presence of low rates of osmotic flow towards the mucosa; for example, in one experiment where 50 m-molal (mM) sucrose was already present in the mucosal solution, addition of glutaraldehyde to both the mucosal and serosal solutions produced a transient streaming potential and a decrease in the width of the extracellular spaces.

Osmium tetroxide had quite different effects. When added to the mucosal solution, it produced a transient (mucosa positive) change in the p.d. across the bladder wall, and the gallbladder resistance dropped towards free solution. This indicates that osmium tetroxide "fixes" cell membranes on contact and in so doing destroys their permeability characteristics. Previous experience (e.g., Tormey & Diamond, 1967) suggests that this fixative also has minimal effects on the volumes of cells and subcellular compartments. Therefore, we regard it as the fixative of choice. Accordingly most of our fixation was carried out in 1% OsO_4 buffered at pH 7.4 in 0.15 M sodium phosphate.

Nonetheless certain artifacts are peculiar to osmium fixation, the most serious being its ability to obliterate intercellular spaces between closely apposed membranes (Tormey, 1964). Because glutaraldehyde prevents this latter sort of artifact, we also fixed at least one of each type of experiment (*see* p. 175) in glutaraldehyde as a control. We used 1 and 3% solutions of vacuum distilled glutaraldehyde in 0.1 M phosphate buffer, followed by a buffer wash and postfixation in osmium tetroxide. The results corroborated

those obtained with osmium, especially in respect to the lateral spaces of the mucosal epithelium. However, the two fixatives produced significantly variant results in the submucosal cores of the mucosal folds of bladders with hypertonic mucosal bathing solutions. With 1% glutaraldehyde the submucosal cells appeared swollen to the point where they occupied about 99% of the volume of the core; with osmium tetroxide and (significantly) with 3% glutaraldehyde they occupied 80 to 95% of the volume. We judge the results with 1% glutaraldehyde to be, in this case, artifactual. Glutaraldehyde fixation, unlike osmium, takes many minutes, during which the cell membrane retains its semipermeability and the cell is able to respond osmotically. Since different cell types in the same tissue can have vastly different reflection coefficients to glutaraldehyde (Grantham & Tormey, *unpublished*), we expect instances where glutaraldehyde has little effect on one cell type while making another cell type swell or shrink.

Following fixation the tissues were dehydrated in ethanol and embedded in Epon 812. Light microscopy was carried out on 0.5 μm thick sections stained with toluidine blue. Thin sections for electron microscopy were stained with uranyl acetate followed by lead citrate.

Results

We have organized the description of the results in the following manner: First we demonstrate the effect of osmotic gradients on nonelectrolyte unidirectional fluxes and pose the question whether or not these results are explained by unstirred layer effects. The second series of experiments are those in which we measure gallbladder resistance to evaluate the effect of osmotic gradients on ion permeability. Next, we show the appearance of the transport number effect in the presence of sucrose gradients and, finally, we describe the osmotically induced changes in the ultrastructure of the gallbladder.

Nonelectrolyte Fluxes

Sucrose fluxes across the gallbladder were measured in the presence and absence of sucrose concentration gradients (Fig. 1). In the absence of gradients, the unidirectional fluxes, J_{ms} (mucosa to serosa) and J_{sm} (serosa to mucosa), were directly proportional to the sucrose concentration over a range of at least 10 to 100 mM. (The proportionality constant corresponds to a permeability coefficient of 4×10^{-6} cm/sec.) In the absence of sucrose from the mucosal fluid J_{sm} was also proportional to the sucrose concentration in the serosal solution. There was no significant difference between the J_{sm} fluxes in the absence or presence of the gradient. In contrast, without sucrose in the serosal fluid, J_{ms} increased in a markedly non-linear fashion with increasing concentration in the mucosal fluid; for example, with 100 mM sucrose, the ratio of J_{ms} without sucrose in the serosal fluid to J_{ms} with sucrose in both solutions was 0.5 ± 0.1 . In other words P_{sucrose} was reduced by about one-half when the mucosal solution was made hypertonic

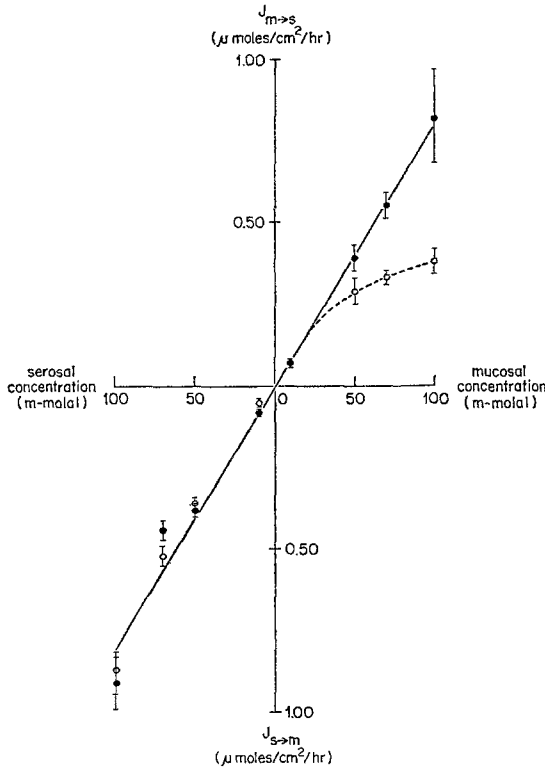


Fig. 1. The effect of osmotic gradients on sucrose fluxes across the rabbit gallbladder. The ordinate is the steady state sucrose unidirectional flux expressed in μ moles/cm²/hr; J_{m_s} and J_{s_m} are the mucosa to serosa and serosa to mucosa unidirectional fluxes, respectively. The abscissa is the sucrose concentration (mM). The fluxes given by the closed circles (•) were obtained in the absence of sucrose concentration gradients, i.e., the mucosal and serosal concentrations were identical, and the open circles (◦) are J_{m_s} and J_{s_m} fluxes in the absence of sucrose in the serosal and mucosal solutions, respectively; i.e., unidirectional fluxes obtained in the presence of adverse osmotic gradients. The bars give the SEM. In each gallbladder the fluxes in the presence of osmotic gradients were bracketed with fluxes in the absence of gradients. In the mucosal to serosal direction each point represents at least fifteen estimates on the flux in at least five gallbladders while the points for the fluxes in the serosa to mucosa direction are the average of at least eight estimates in at least two gallbladders

with respect to the serosal solution. In additional experiments at even higher sucrose concentrations (300 mM), P_{sucrose} was reduced by about 75%.

This distinct asymmetrical behavior was further investigated by measuring other nonelectrolyte fluxes across the gallbladder with sucrose present in either the mucosal or serosal fluids. Such an experiment is shown in Fig. 2 where we measured 1,4-butanediol fluxes across the gallbladder. There was no apparent change in the 1,4-butanediol flux from the mucosal

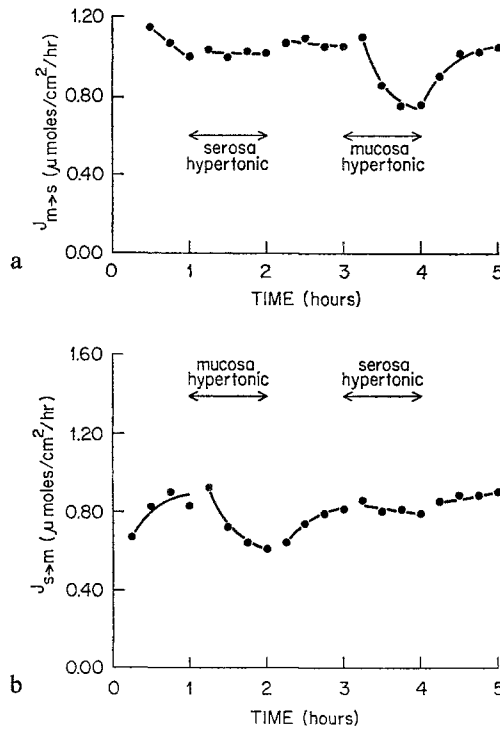


Fig. 2 a and b. The effect of osmotic gradients on 1,4-butanediol unidirectional fluxes across the gallbladder. Shown are two separate experiments; the upper is the flux in the mucosal to serosal direction, and the lower is the flux in the serosal to mucosal direction. In each the flux ($\mu\text{moles}/\text{cm}^2/\text{hr}$) is plotted as the ordinate against time as the abscissa. The 1,4-butanediol concentration was 10 mM in both the mucosal and serosal fluid throughout, and at the times indicated the mucosal or serosal solutions were replaced with sucrose (40 mM) or sucrose-free solutions. Apart from sucrose the composition of the mucosal and serosal solutions were identical throughout the experiments

to the serosal fluids when the serosal fluid was made hypertonic, but there was a significant decrease when the mucosal fluid was made hypertonic (Fig. 2a). The flux decreased with a half time of about 15 min and the effect was reversible when the mucosal fluid was replaced with sucrose-free saline. In Fig. 2b it can be seen also that the serosal to mucosal flux was reduced by the addition of sucrose to the mucosal fluid but that the flux was unaffected by sucrose in the serosal fluid. Both the time course and the magnitude of the reduction in J_{sm} and J_{ms} 1,4-butanediol fluxes were very similar. Additional experiments were carried out where we added either 100 or 300 mM sucrose to the mucosal fluid and we found that the 1,4-butanediol fluxes were reduced by about 50 and 75%, respectively. Thus, at the same osmotic gradients there was the same percentage decrease in

the sucrose and 1,4-butanediol fluxes (compare for example, Figs. 1 and 2). Similar experiments were also carried out with urea, acetamide and 1,7-heptanediol; for example, in one experiment the fluxes of sucrose, acetamide, 1,4-butanediol and 1,7-heptanediol were reduced by about 85% upon addition of 300 mM sucrose to the mucosal fluid.

In summary, making the mucosal solution hypertonic caused a decrease in the permeability of the gallbladder to a variety of nonelectrolytes. The reduction was independent of the direction of the unidirectional fluxes; i.e., under any osmotic gradient the two unidirectional fluxes, J_{sm} and J_{ms} , were always identical. The permeabilities of all solutes studied were reduced to a similar degree. Owing to experimental errors, scatter in the results, and the relatively small effect, we cannot conclude whether there were significant differences among the nonelectrolytes. In contrast, making the serosal solution hypertonic had no measurable effect on nonelectrolyte permeation.

Contribution of Solute-Solvent Interactions

These osmotic effects might be explained, in principle, by solute-solvent interactions. Indeed, the initial purpose of these experiments was to continue our studies of nonelectrolyte permeability (Smulders & Wright, 1971) by evaluating the magnitude of such interactions in the gallbladder.

One such interaction is the sweeping effect of water flow, which, depending on its direction, can enhance or deplete the solute concentration in the unstirred layers adjacent to the membranes. In this way, water flow can alter the local concentration gradient across the membrane and thereby change the flux. The relationship between water flow and the concentration of solute adjacent to the membrane (C_m), is given by

$$C_m = C_b e^{\left(\frac{V\delta}{D}\right)}$$

where C_b is the concentration of solute in bulk solution, V is the velocity of water flow, δ the unstirred layer thickness, and D the solute free solution diffusion coefficient (Dainty, 1963). Since the unstirred layer on the serosal side of the gallbladder is $\sim 800 \mu$ thick, whereas the mucosal unstirred layer is only $\sim 100 \mu$ thick (Smulders & Wright, 1971), almost all the effect will arise on the serosal side¹. Therefore, the principle effect of water flow from

¹ The thickness of the unstirred layers is the effective thickness assuming that diffusion coefficients in the unstirred layers are identical to those in free solution (see Smulders & Wright, 1971; and Paper 2 for further details).

mucosa to serosa will be a tendency to change the concentration of permeating solutes on the serosal side of the epithelium. If the solute is permeating from the mucosal side, the effect obviously will enhance the gradient and increase J_{ms} ; if it is permeating from the serosal side, the gradient will be reduced and J_{sm} will fall. Similar considerations apply to water flow in the opposite direction. The fact that $J_{ms} = J_{sm}$ in all cases shows that this unstirred layer effect must be negligible.

Theoretical considerations also indicate the unstirred layer effects should be similar in magnitude regardless of the direction of water flow. It is, therefore, significant that flow from serosa to mucosa has a marked effect on permeability, while flow in the opposite direction has none. Calculations verify that unstirred layer contributions to altered gallbladder permeability must be small. For example, 100 mM sucrose added to the serosal fluid will produce at most a 10% change in sucrose flux: i.e., $e^{(-V \delta_s/D)} = 0.9$, where $V = 6 \times 10^{-6}$ cm/sec (from Table 1, Paper 2), $\delta_s = 800 \times 10^{-4}$ cm, and $D_{\text{sucrose}} = 5.2 \times 10^{-6}$ cm²/sec.

Solute-solvent interactions within the membranes themselves also fail to account for our observations. Solvent drag, like unstirred layers, must produce asymmetrical effects. For example, while water flow towards the mucosa would reduce J_{ms} by frictional interaction, it should likewise enhance J_{sm} to a similar degree. This clearly does not occur in our experiments.

Resistance Changes

Previously (Wright & Diamond, 1968; Wright, Barry & Diamond, 1971), it was shown that the resistance of the rabbit gallbladder is about $28 \Omega \text{ cm}^2$ and that at least 94% of the tissue resistance was provided by the epithelium alone. Fig. 3 shows the change in the gallbladder resistance upon addition of sucrose (100 mM) to the mucosal fluid. The resistance increased from 30 to 68 Ω with a half time of about 9 min. The magnitude of the resistance change depends on the reflection coefficient of the solute used to increase the osmolarity of the mucosal fluid; for example, addition of *n*-butyramide ($\sigma \sim 0.5$) to the mucosal fluid only produced about half the increase in resistance produced by the same concentration of sucrose ($\sigma = 1$).

The magnitude of the resistance change was also concentration dependent. This is shown in Fig. 4 where we have plotted gallbladder conductance ($1/R$) against the sucrose concentration in the mucosal and serosal solutions. Increasing the sucrose concentration in the mucosal fluid resulted in a

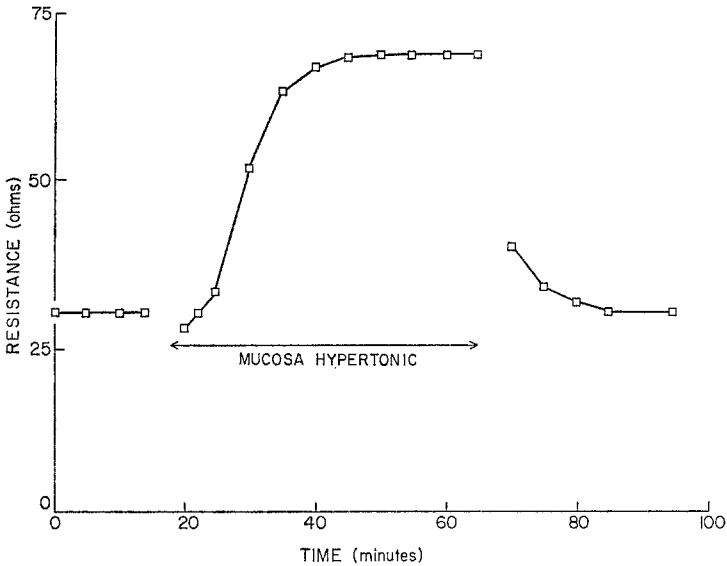


Fig. 3. The increase in the gallbladder resistance on addition of sucrose to the mucosal fluid. Gallbladder resistance (Ω) as the ordinate is plotted against time on the abscissa. At the times indicated the mucosal solution was replaced with sucrose (100 mM) or sucrose-free solutions; the composition of the solutions, apart from sucrose, remaining identical. The subsequent addition of sucrose to the serosal fluid (not shown) produced no change in the resistance of this or any other gallbladder

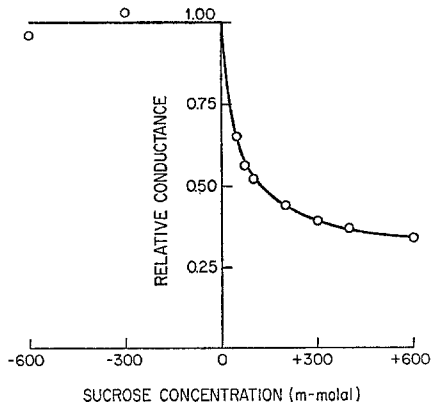


Fig. 4. Conductance of the gallbladder as a function of the sucrose concentration in the mucosal and serosal solutions. The conductance, on the ordinate, is the conductance relative to the average value obtained in sucrose-free solutions before and after the exposure to sucrose. The sucrose concentration, on the abscissa, is positive when sucrose is present in mucosal solution and absent from the serosal solution, and is negative when the sucrose is in the serosal solution but absent from the mucosal solution. All points were obtained from the same gallbladder preparation

progressive decrease in the tissue conductance which leveled off at about one-third of the control value. The half time for the resistance change decreased with increasing sucrose concentration, such that at 300 mM the half time was about 4 min (*see also* Paper 2). In six gallbladders, the conductance was reduced to $61 \pm 2\%$ and $29 \pm 1\%$ of the normal value on addition of 50 and 300 mM sucrose, respectively, to the mucosal fluid.

In contrast to the effect of sucrose in the mucosal fluid, there was no change in the tissue resistance when (1) sucrose was added to the serosal fluid (Fig. 4), and (2) when sucrose was added to both the mucosal and serosal fluids. Furthermore, the changes in resistance produced by sucrose in the mucosal fluid were reversed by the subsequent addition of sucrose to the serosal fluid.

Both nonelectrolyte fluxes and tissue conductance were reduced in about the same proportion on addition of sucrose to the mucosal fluid but neither were affected by sucrose in the serosal fluid. For example, in one gallbladder the flux of 1,4-butanediol and the tissue conductance were both reduced by 50% when sucrose (100 mM) was added to the mucosal fluid (compare also Figs. 1 and 4) and in two other experiments the 1,4-butanediol flux and electrical conductance were reduced by 60 and 70%, respectively, upon addition of 300 mM sucrose to the mucosal fluid.

Osmotically induced changes in tissue conductance have also been observed by Frömter and Lürer (1969) in the proximal tubule of the rat kidney, by Frömter (*personal communication*) in *Necturus* gallbladder and by us in frog gallbladder, frog choroid plexus and rabbit ileum. In general, these results are qualitatively very similar to those described for the rabbit gallbladder, i.e., osmotic flows towards the mucosa are associated with an increase in resistance whereas flow in the opposite direction is associated with either no change or a fall.

To check that changes in the gallbladder conductance are largely equated with changes in sodium permeability as predicted from other considerations (*see* Wright *et al.*, 1971; Barry, Diamond & Wright, 1971), we carried out an experiment where we measured unidirectional sodium fluxes (J_{Na}), conductances and sodium chloride diffusion potentials both in the presence and absence of osmotic gradients. There was no significant difference between the sodium permeability coefficients obtained from flux measurements or calculated from the electrical parameters (*see also* Diamond, 1962). In the absence of osmotic flows, the radioactive tracer permeability coefficient was 3×10^{-5} cm/sec, whereas P_{Na} estimated from the diffusion potentials and tissue conductance was 4.5×10^{-5} cm/sec. I.e., $P_{Na} = \frac{G_{Na} RT}{F^2 C_{Na}} = 4.5 \times 10^{-5}$ cm/sec, where $G_{Na} = \left(\frac{1.0}{1.0 + P_{Cl}/P_{Na}} \right) G$, $P_{Cl}/P_{Na} = 0.2$, $G = 31 \times 10^{-2}$ mho/cm², R the gas constant, T absolute temperature, F the Faraday and C_{Na} the sodium concentration. There was also good agreement between the

osmotically induced decrease in the tissue conductance and the sodium flux; the unidirectional sodium flux and the tissue conductance were reduced by 50 and 40%, respectively, upon addition of sucrose (100 mM) to the mucosal fluid. This experiment suggests that there is little or no active transport or exchange diffusion of sodium across the gallbladder under the conditions of the experiment, and it shows that gallbladder conductances are largely accounted for by sodium fluxes.

Arguments similar to those used on p. 170 rule out unstirred layer effects and solvent drag as possible explanations for osmotically induced changes in ion permeability.

Polarization Potentials

When direct current was passed across the gallbladder in the absence of osmotic gradients, or with hypertonic serosal solutions, the potential assumed a new steady state value within the time response of the recorder (ca. 1 sec), and, at the current densities employed ($<200 \mu\text{amp}$), the p.d. remained stable as long as the current was applied. However, when the mucosal solution was made hypertonic a polarization p.d. became apparent, particularly when the resistance had reached the steady state value. The sign of the polarization was in the same direction as the IR step, the half time for the build up and decay of the polarization p.d. was about 25 sec, and the effect was more pronounced when the serosal solution was made electrically positive than when the mucosal solution was made positive. With 100 mM sucrose in the mucosal solution, the polarization p.d. was up to 1.5 mV when 100 μamp was passed across the tissue, and the size of the p.d. increased with increasing sucrose concentration. These polarization p.d.'s are probably due to the transport number effect (*see Barry & Hope, 1969a, 1969b; Wedner & Diamond, 1969; Wright et al., 1971*).

Another phenomenon associated with the appearance of the transport number effect is current-induced resistance changes. In the absence of osmotic gradients, the IR steps obtained by switching the current on and off were identical as expected for a simple ohmic resistor. However, with hypertonic mucosal solutions the IR step on switching the current on was either a few percent smaller (with the current oriented to make the serosal solution positive) or larger (with the current in the reverse direction) than the IR step obtained when the current was switched off. The discrepancy between the IR steps must be caused by resistance changes as the current was passed across the gallbladder.

Tissue Structure Changes

To determine how changes in tissue structure might be related to the osmotically induced permeability changes described above, we examined gallbladders under various conditions of osmotic water flow. Namely:

(1) *Absence of Osmotic Water Flow.* The aim of this group of experiments was to determine structure at zero flow, to learn whether structure is essentially independent of bathing solution osmolarity, and to establish that osmotically induced changes are reversible. Three sorts of experiments were therefore done: (i) The mucosal solution was made hypertonic with 300 mM sucrose. After the resistance change was complete, the mucosal solution was returned to normal (sucrose-free) saline. The tissue was fixed once resistance returned to control level (2 bladders). (ii) Same as above, except that, after exposing the mucosal surface to 300 mM sucrose, both the mucosal and serosal solutions were replaced with saline containing 150 mM sucrose (1 bladder). (iii) Without first applying a gradient, both the mucosal and serosal solutions were made hypertonic with 150 mM sucrose, and the tissue was fixed 30 min later (1 bladder).

(2) *Osmotic Flow from Mucosa to Serosa.* Following the control period, the serosal solution was made hypertonic with 300 mM sucrose. The tissue was fixed 30 min later (3 bladders).

(3) *Osmotic Water Flow from Serosa to Mucosa.* (i) The mucosal solution was replaced with saline with 300 mM sucrose added. Fixation was begun after the resistance change was complete (4 bladders). (ii) Same as above, except that the mucosal solution was made hypertonic by only 50 mM sucrose (4 bladders).

In all but one experiment (1, iii) there was an initial control period of 45 min, during which the bladders were bathed in normal Ringer's solution on both surfaces, and control levels of electrical resistance were determined.

Water flows were found to produce dramatic changes in the dimensions of extracellular spaces, not only of the epithelium, but also of the rest of the gallbladder wall (*see* Fig. 5 for a summary of the anatomy of the gallbladder wall).

Light Microscope Observations

Epithelium. Water flow from mucosa to serosa produced extreme dilation of the lateral intercellular spaces to widths averaging well over 1 μm (Fig. 6*a*). The widest spaces were consistently found on the tips of the mucosal folds. In the absence of an osmotic gradient, these spaces collapsed to about 0.3 μm width, i.e., they could barely be discerned by light microscopy (Fig. 6*b*). These results are identical to those found previously (Tormey & Diamond, 1967) with active fluid transport.

Water flow from serosa to mucosa caused further collapse of intercellular spaces to the point where they were completely undetectable by light microscopy (Fig. 6*c*). This was true regardless of the size of the gradient (50 or 300 mM).

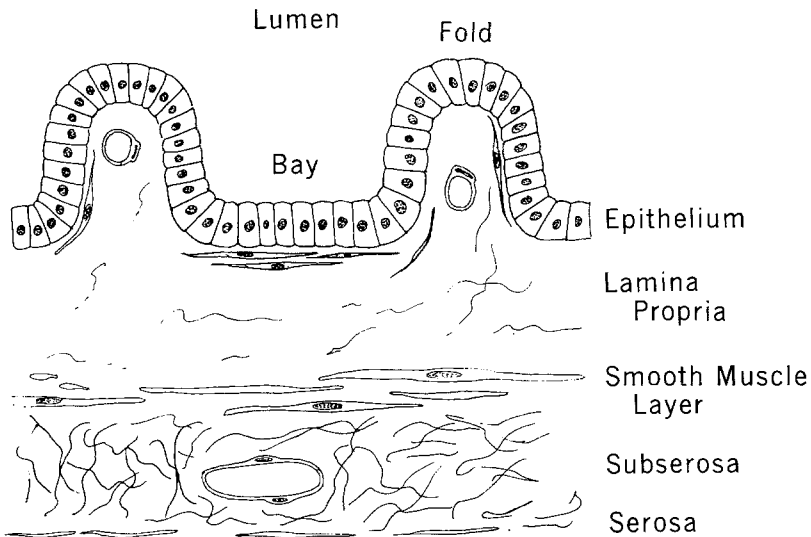


Fig. 5. Diagram illustrating the salient features of the gallbladder wall. The Lamina propria is referred to in the present paper as the *submucosa*. Not drawn to scale. (From Tormey & Diamond, 1967; *q.v.* for further anatomical details)

No changes in cell volume could be detected among the foregoing experiments, in spite of the fact that three observers made measurements of cell height and width with an eyepiece screw micrometer. However, the structure of the epithelium was so variable that volume changes on the order of up to 20% might easily have been missed. At any rate, this implies that the water permeabilities of the apical and basal-lateral epithelial membranes are of the same order of magnitude.

Submucosa. Marked differences were also found in the rest of the bladder wall (*cf.* Fig. 7). As summarized in Table 1, the large variations in its overall width were due mainly to changes in the submucosa. In the absence of water flow the submucosa looked "normal", i.e., the various connective tissue elements were loosely organized and separated by large, apparently empty spaces. Flow towards the serosa caused the submucosa to swell to nearly four-times its resting width, with a corresponding increase in separa-

Fig. 6 a-c. High power light micrographs of mucosal folds of rabbit gallbladders. Three osmotic water flow conditions are represented: (a) mucosa to serosa flow with the serosal solution hypertonic by 300 mM; (b) zero flow with both bathing solutions hypertonic by 150 mM; (c) serosa to mucosa flow with mucosal solution hypertonic by 300 mM. The mucosal epithelium has widely dilated lateral intercellular spaces (*lis*) in (a); narrow barely discernable spaces in (b); no detectable spaces in (c). The cores of the folds (*cf*) are similarly widely dilated, open, and closed. 0.5 μm thick sections. 675 \times

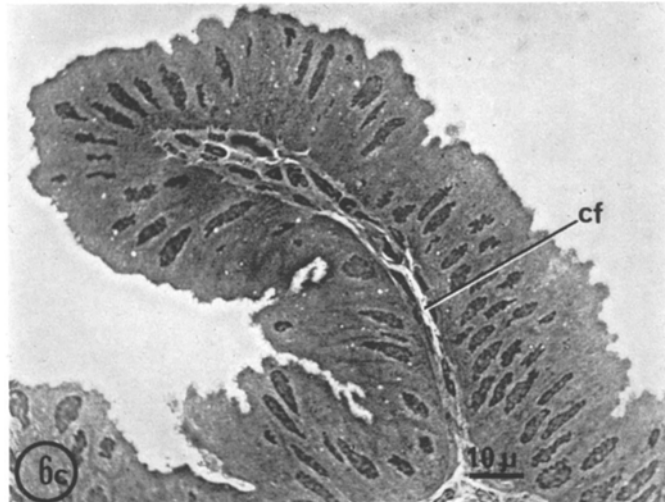
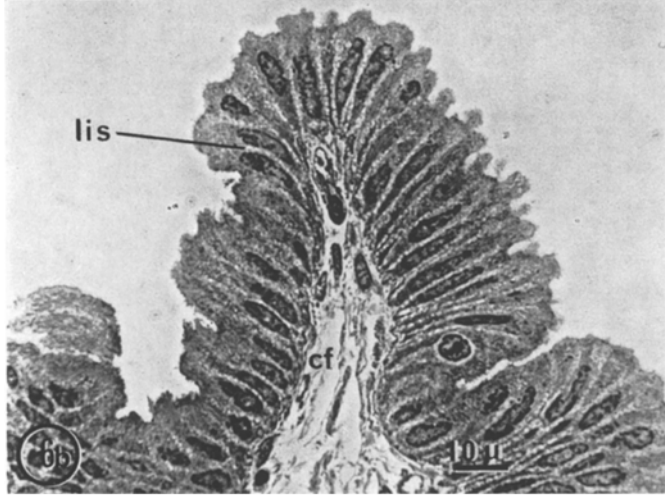
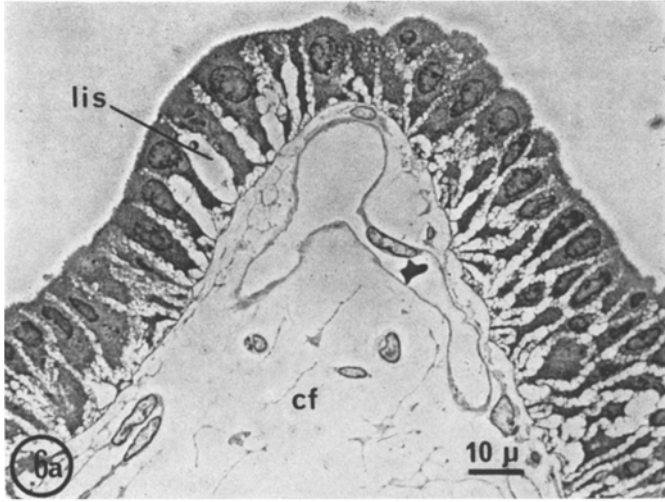


Fig. 6a-c

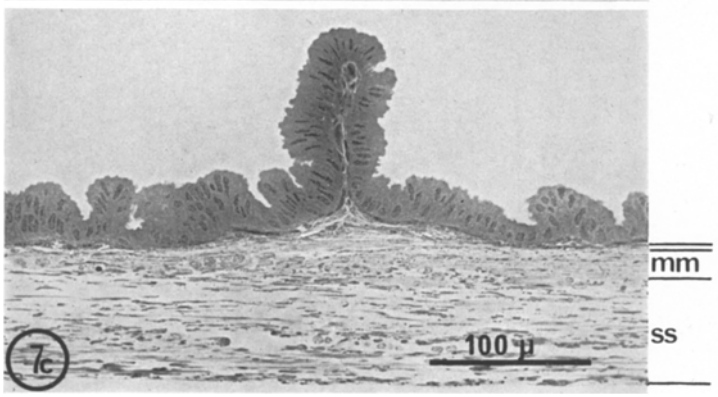
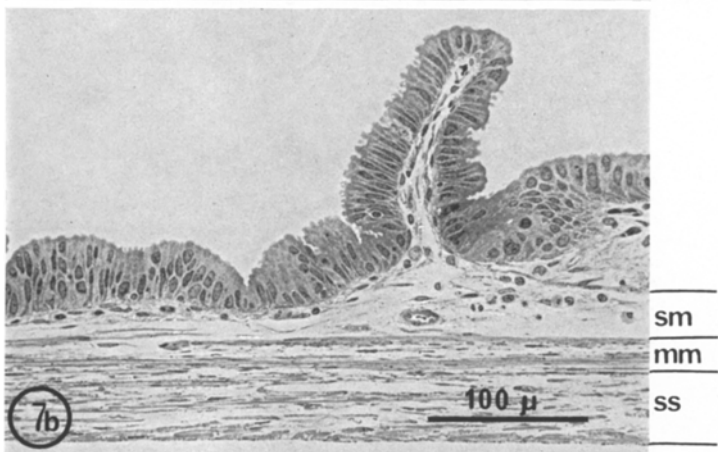
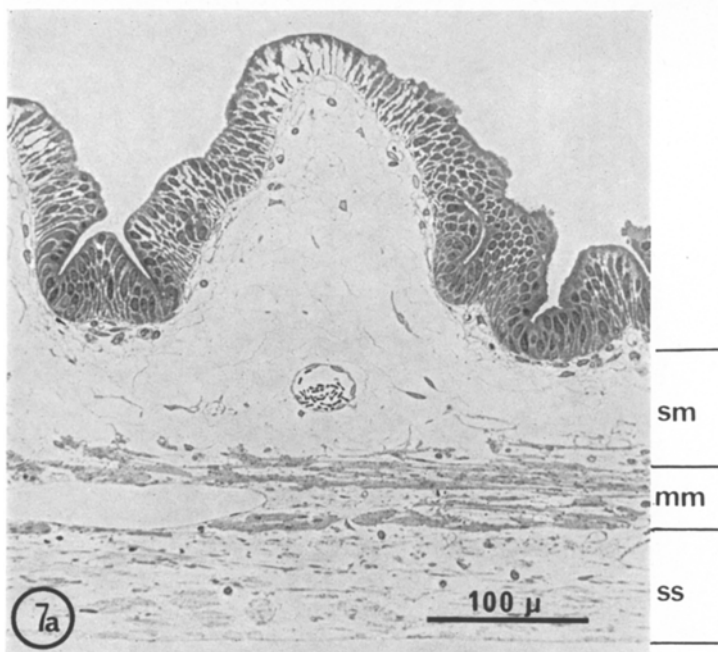


Fig. 7 a-c

Table 1. Widths of components of gallbladder wall

	Whole wall (excluding epith.) μm	Submucosa μm	Muscularis μm	Subserosa μm
$\Delta\pi = 300$ serosa	208 (± 9)	113 (± 22)	51 (± 5)	44 (± 13)
$\Delta\pi = 0$	114 (± 34) ^a	30 (± 9)	35 (± 7)	50 (± 23)
$\Delta\pi = 300$ mucosa	60 (± 17)	~ 0	23 (± 4)	35 (± 14)

The above figures are arithmetic means and standard deviations. Each is calculated from mean widths measured on either three or four separate gallbladders. The widths of each individual bladder were in turn computed from several measurements made at representative points. (The variation between individual bladders was in general much greater than between different regions of the same bladder.) Measurements were made with $25\times$ objective. Measurements of submucosa width in $J_{s \rightarrow m}$ experiments are underestimated because of difficulty in distinguishing compact submucosa from muscularis at this magnification.

^a Note that these wall widths are less than those reported previously for sac preparations (Tormey & Diamond, 1967). The difference is due to the fact that our present preparations are stretched when mounted between chambers.

tion of structural elements. Flow towards the mucosa produced a correspondingly great shrinkage, such that the cellular elements became closely crowded together with but small spaces between them.

The submucosal folds varied accordingly. They ranged from very broad and empty with water flow towards the serosa, to extremely narrow and compacted with flow in the opposite direction. The proportion of the epithelial cell population located on folds varied from nearly 100% when the folds were greatly expanded to about 50% in all other cases. Typically, the submucosal "core" of a fold collapsed by 300 mM sucrose on the mucosa was about 90 μm long by 5 μm wide. With 50 mM sucrose on the mucosa the folds were somewhat wider.

Folding (exclusive of microvilli) increased the effective surface area of the mucosa by a factor of about $1.5\times$. Somewhat surprisingly, this factor

Fig. 7 a-c. Lower power light micrographs of the entire thickness of the gallbladder wall. Osmotic water flow conditions are identical to those in Fig. 6: i.e., (a) is mucosa to serosa flux, (b) is zero flow, (c) is serosa to mucosa flow. The dimensions of the bladder wall vary with water flow. The largest alterations are in the thickness and degree of packing of the submucosa (*sm*). The muscularis mucosa (*mm*) also varies its thickness and packing, though to a lesser degree. The thickness of the subserosa layer (*ss*), while rather variable, does not correlate with water flow conditions. (Cf. also Table 1.) Small blood vessels are dilated in (a), open in (b), undiscernable in (c). $215\times$

remained essentially constant in all experiments, except for an increase to about $1.7 \times$ with flow towards the serosa.

Muscularis. The width of the smooth muscle layer varied consistently but less dramatically from about $50 \mu\text{m}$ during mucosa to serosa water flow to about $25 \mu\text{m}$ found during reverse flow. As suggested by Fig. 7 this difference was due to differences in packing of muscle cells: they were very loosely arranged with wide intercellular spaces in the one case and extremely close together in the other. Zero flow and low serosa to mucosa flow conditions gave an intermediate appearance.

Subserosa. This region, consisting mainly of loosely interwoven bundles of collagen, is one which did not vary consistently from one situation to another. It was, however, quite variable in width from bladder to bladder, and this accounts for most of the variability in wall widths found in each experimental category.

Electron Microscope Observations

Electron microscopy added information about the "closed" spaces between cells. In the absence of osmotic water flow, the lateral intercellular spaces were about $0.6 \mu\text{m}$ wide (Fig. 8*a*). Cytoplasmic evaginations about $0.1 \mu\text{m}$ in diameter and $1 \mu\text{m}$ long protruded into this space and loosely interdigitated with one another. They partially occluded the space to varying degrees; in different preparations the amount of occlusion varied from

Fig. 8*a-c*. High magnification electron micrographs showing details of the lateral intercellular spaces. (*a*) depicts zero water flow conditions. The channel is roughly $0.7 \mu\text{m}$ wide, but is effectively narrowed by numerous cytoplasmic folds or evaginations which loosely interdigitate across the channel. (*b*) depicts an area of *maximal* channel closure produced by serosa to mucosa flow under a 300 mM gradient. The cytoplasmic evaginations are tightly interdigitated. The intercellular channel appears to be patent in only a few places. The offset square indicates a typical area similar to the one shown at higher magnification in Fig. 9. (*c*) shows a less extreme degree of channel closure, produced by serosa to mucosa flow under only a 50 mM gradient. Though tightly closed compared to (*a*), in no place is the channel completely closed. Average channel width here is on the order of $0.02 \mu\text{m}$. All $36,000 \times$

Fig. 9. $126,000 \times$ micrograph of region with tightly closed channels, similar to that depicted in Fig. 8(*b*). Detail is somewhat obscured because thickness of section ($\sim 80 \text{nm}$) is much greater than the dimensions of the details being resolved. Nevertheless, the typical trilaminar structure of the "unit" plasma membrane is evident. In a few places (*o*), the intercellular space is seen to be narrowly open. In a few other places (*c*), the intercellular space appears to be completely obliterated and the apposed unit membranes take on a pentalamellar appearance reminiscent of tight junctions

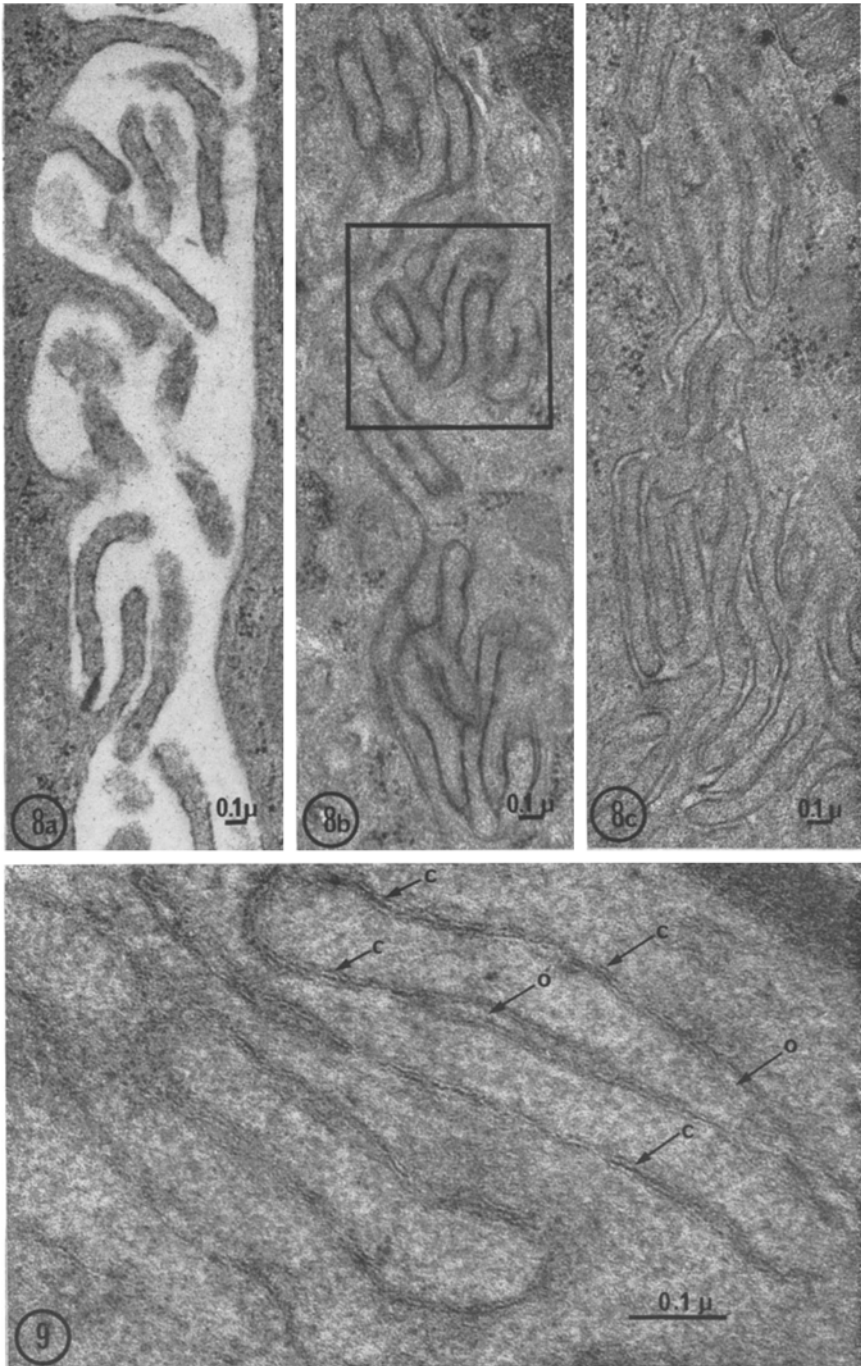


Fig. 8 a-c and Fig. 9

about 35 to 75%. Hence, the effective width of the spaces was on the order of 0.3 μm . These lateral channels were collapsed as compared with the widely dilated spaces associated with mucosa-to-serosa flows (*cf.* Tormey & Diamond, 1967), but were wide open in comparison to those found with reverse flows.

The intercellular spaces of gallbladder with 300 mM sucrose added to the mucosal side were more than an order of magnitude tighter (Fig. 8*b*). In fact, the intercellular space often appeared completely obliterated. For example, Fig. 9 shows the adjacent plasma membranes of interdigitating cytoplasmic evaginations to be intimately associated in "pentalaminar" structures reminiscent of tight junctions. These are probably not fixation artifacts, since they were found alike in bladders fixed in osmium tetroxide or glutaraldehyde, but neither are they typical tight junctions. They seem to be simply regions where the intercellular spaces were dehydrated and collapsed to the point where the cell membranes either actually touched or were separated by gaps only a few water molecules wide. A somewhat similar though less extreme appearance has been described by Berridge and Gupta (1967) for certain paired membranes in rectal papillae under conditions of minimal fluid transport. These areas of intimate membrane apposition occupied about half of the lateral surface area of the cells, alternating with areas where cell membranes were separated by a gap averaging 10 nm (100 Å) wide.

The intercellular spaces of bladders with only 50 mM sucrose on the mucosa were also tightly closed. However, there were very few areas where the membranes were in close contact. The intercellular spaces averaged 18 nm (180 Å) in width (Fig. 8*c*).

No changes in tight junction structure have been detected in these experiments. Since there is increasing evidence that the junctions are a major route of permeation across the gallbladder epithelium (*see* p. 187) it is *a priori* possible that water flow might alter epithelial permeability by modifying this structure. For this to be the case, the structure would have to be asymmetrical so that water flows from serosa to mucosa would effectively increase the resistance of this pathway, whereas water flow in the opposite direction would have no effect. The corresponding change in structure could take two forms: (1) an increase in the length of the junction, or (2) microchannels in the junction might collapse. Although the first should be easy to visualize it is not observed. The second would be difficult to detect since there are no techniques available for resolving channels in junctions clearly.

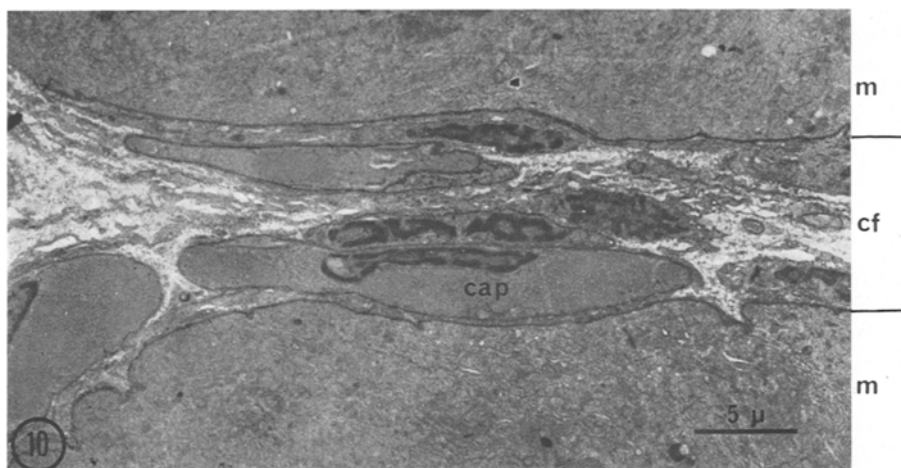


Fig. 10. Low power electron micrograph depicting the core of a mucosal fold under conditions of maximal serosa to mucosa water flow. The core of the fold (*cf*) here runs from left to right, flanked above and below by the bases of epithelial cells (*m*). The space on the left-hand side is funneling down as the fold begins; thereafter the width of the core remains relatively constant. *cap* represents a completely collapsed capillary. The amount of extracellular space in the fold is quite variable, but averages at least 5% of the total. $2,750\times$

Certain subepithelial regions of close-packed structure were also examined. With 300 mM sucrose on the mucosal side about 95% of the submucosal cores of the mucosal folds were occupied by cells and collagen, leaving about 5% open area (Fig. 10). With a 50 mM gradient, the total open area increases to about 20%. (These results were obtained with tissue fixed in either osmium tetroxide or 3% glutaraldehyde; see p. 167.)

Packing of tissue elements elsewhere in the submucosa and in the muscularis was much less regular and consistent, with close-packed areas interspersed with loosely organized ones. Even in the most closely packed muscle layers, 15% of the volume was intercellular space (Fig. 11).

To summarize, these anatomical studies show that the extracellular spaces of the epithelium, the submucosa, and muscularis dilate during osmotic flow from the mucosa to serosa and that spaces collapse during flow in the opposite direction. To determine whether these changes explain the effects of osmotic gradients on permeability we must calculate whether or not the spaces become narrow enough to become rate limiting. These calculations also enable us to evaluate the relative importance of changes in spaces within the epithelium and in the rest of the gallbladder wall. As a

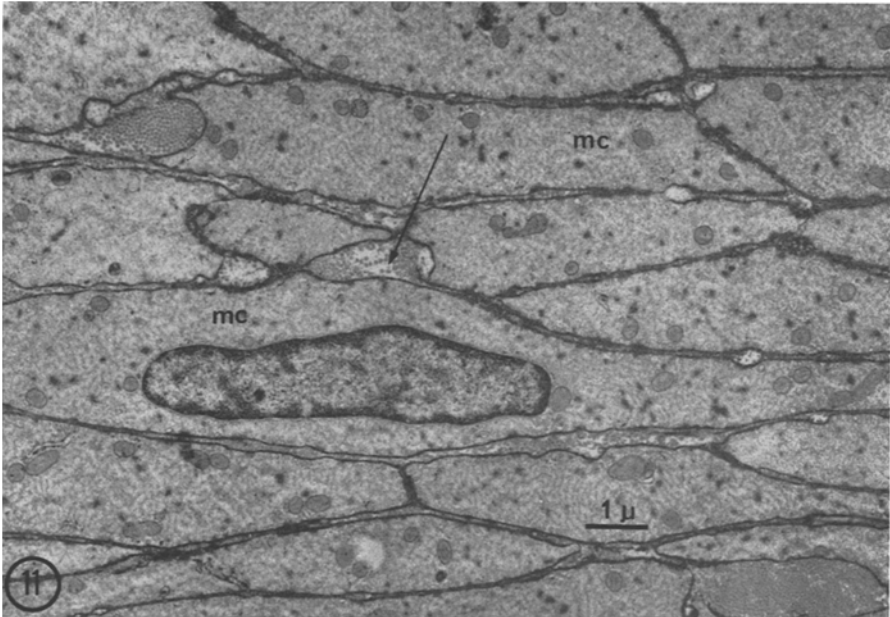


Fig. 11. Low power electron micrograph of a particularly tightly closed region of the muscularis mucosa, produced by a maximal serosa to mucosa water flow. Between the individual muscle cells (*mc*), here cut obliquely, there are considerable widths of extracellular space. These spaces are much wider than those of the overlying epithelium. The extracellular spaces are partially filled with varying amounts of collagen. $8,000\times$

starting point Table 2 summarizes the relevant dimensions of the epithelium, mucosal folds and muscularis under various experimental conditions.

Osmotically induced changes in lateral intercellular spaces have been described in other epithelial membranes; in frog intestine (Loeschke, Bentzel & Csáky, 1970), *Necturus* proximal tubule (Bentzel, Parsa & Hare, 1969), rabbit renal collecting duct (Grantham, Ganote, Burg & Orloff, 1969), blowfly rectal papillae (Berridge & Gupta, 1967) and in amphibian urinary bladder (Grantham *et al.*, 1971). These workers observed that spaces dilate with osmotic flows directed towards the serosa.

Discussion

A striking feature of the results is the asymmetrical behavior of the isolated rabbit gallbladder. Increasing the osmolarity of the mucosal fluid reduces the permeability of the tissue to both ions and nonelectrolytes whereas increasing the osmolarity of the serosal fluid produces no dis-

Table 2. Parameters for estimating effect of structure on permeability

	$\Delta\pi = 0$	$\Delta\pi = 50$ mucosa	$\Delta\pi = 300$ mucosa
<i>Epithelium (intercellular space)</i>			
Height of cells ^a ($\times 10^4$ cm)	30	60	60
Width of intercellular space ($\times 10^7$ cm)	300	18	10
Cellular circumference ($\times 10^{-3}$ cm/cm ² , cell surface)	8 ^b	40 ^c	20 ^d
Area of intercellular space ($\times 10^3$ cm ² /cm ² epithelium) ^e	120	36	10
<i>Submucosal Folds ("core")</i>			
Height of folds ($\times 10^4$ cm)	90	90	90
Open width of fold ^f ($\times 10^4$ cm)	12	1	0.25
Open area of folds ($\times 10^3$ cm ² /cm ² epithelium) ^g	96	8	2
<i>Muscularis</i>			
Height (thickness) of layer ^a ($\times 10^4$ cm)			50
Area of intercellular space ($\times 10^3$ cm ² /cm ² epithelium)			100

These parameters are derived from measurements on light and electron micrographs, most of which are cited in the text. As indicated in footnotes, the raw measurements have been modified to take into account such geometric features as anatomical tortuosity. In calculating the permeability changes attributable to each structure, the two parameters actually used are "height" and "area" per cm² epithelium). Other parameters are listed only because they form the basis for estimating the area.

^a Effective height. The tortuosity of the path between cells is increased by impinging cellular elements, e.g., interdigitations, to such an extent in some cases that the effective length of the path is increased twofold.

^b Cell diameter 5×10^{-4} cm.

^c The increase in the effective cell circumference is due to development of tight interdigitations.

^d Effective circumference is here down because intercellular space is 50% occluded.

^e Width of intercellular space \times cellular circumference $\times 1/2$.

^f I.e., average width of that fraction of a fold which is unoccupied by cells or collagen fibers.

^g Open width of fold $\times 80$ cm/cm² (running length of folds per unit area of mucosa).

cernable effect. The reduction in the gallbladder permeability upon raising the osmolarity of the mucosal solution must be due to the osmotic gradient across the tissue, since the magnitude of the effect is proportional to the effective osmotic pressure generated by the solute used to make the solution hypertonic (see p. 171) and because there are no permeability changes associated with raising the osmolarity of both the mucosal and serosal fluid simultaneously. The permeability changes, which must be related to the osmotic flow of water from the serosa to the mucosa, cannot be due either to solvent drag or sweeping away effects since both predict results which are contrary to those actually observed; for example, both effects predict a

decrease in the unidirectional flux which is opposite in direction to the water flow, and an increase in the unidirectional flux which is in the same direction as the water flow. A clue to the mechanism of the permeability changes comes from the observation that the fluxes of a diverse range of solutes (sodium, sucrose, urea, acetamide, 1,4-butanediol and 1,7-heptanediol) are reduced in approximately the same proportion, i.e., there is no significant difference in their relative permeabilities in the face of a reduction in the absolute permeability coefficients. These six solutes are expected to cross the gallbladder epithelium by at least three separate pathways; via the membrane lipids (e.g., 1,4-butanediol), membrane pores (e.g., urea), and tight junctions (e.g., sucrose and sodium) (*see* Wright & Diamond, 1969*b*; Barry *et al.*, 1971; Smulders & Wright, 1971; Frömter & Diamond, 1972). Thus, it is unlikely that osmotic gradients produce any specific alterations in the cell membranes and tight junctions at the molecular level. The simplest tenable interpretation is that hypertonic mucosal solutions cause an effective reduction in the area of the gallbladder membranes available for permeation.

Our anatomical studies have revealed a structural basis for this change in effective area. We have shown that osmotic flows from the serosa to mucosa are associated with the collapse of the extracellular spaces in the epithelium, submucosa and muscularis. On the other hand, osmotic flow from the mucosa to serosa causes a dilation of these spaces. The question then arises whether the changes in the morphology of the gallbladder wall during osmotic flow explain the permeability changes. In other words, are the structural changes sufficient to explain the physiological observations? To answer this question we have attempted to reconstruct the changes in permeability from the changes in tissue geometry.

The Quantitative Correlation between the Structural and Functional Changes

Permeation Pathways

A discussion of possible permeation pathways across the gallbladder must precede the quantitative correlations. Both ions and nonelectrolytes may permeate across the epithelium by two separate pathways: (1) Solute may by-pass the epithelial cells completely and permeate directly into the lateral spaces from the mucosal solution through the so-called "tight" junctions. The lateral spaces and the remainder of the subepithelial tissues then are diffusion barriers in series with the permeability barrier of the tight junctions, i.e., $1/P_{gb} = 1/P_{\text{tight junction}} + 1/P_{\text{lateral space}} + 1/P_{\text{wall}}$; (2) The alternative pathway is the transcellular route where solutes pass from one side of the epithelium to the other through the epithelial cells, traversing, in

turn, the apical and lateral-basal membranes of the cell. In this case the equivalent circuit is more complex owing to the fact that solutes may exchange between the cell and the lateral spaces along the whole length of the channel, i.e., $1/P_{gb} = 1/P_{\text{apical membrane}} + 1/P_{\text{lateral membrane/lateral space}} + 1/P_{\text{wall}}$. There is a considerable array of evidence to suggest that sucrose (Smulders & Wright, 1971) and ions (Barry & Diamond, 1970; Barry *et al.*, 1971; Wright *et al.*, 1971; and Frömter & Diamond, 1972) permeate across the gallbladder via the tight junctions. For example, in the *Necturus* gallbladder more than 95% of the passive ion flux passes across the tight junctions (Frömter & Diamond, 1972). In the case of lipid soluble nonelectrolytes such as 1,4-butanediol it is likely, although as yet unproven, that these solutes permeate via the cellular pathway (*see* Smulders & Wright, 1971).

Predicted Permeability Coefficients

The principle behind the calculations used to predict the permeability from the changes in tissue geometry is to compute the "permeability" of the lateral spaces, submucosa and muscularis from the relationship

$$P = DA/l$$

where P is the permeability coefficient, D the free solution diffusion coefficient, and A and l are the effective area and length of each component of the diffusion pathway, and to insert these permeability coefficients into the appropriate equivalent circuit. Similar computations were carried out for the electrical conductance (G) using the relationship

$$G = kA/l,$$

where k is the specific conductance of a 0.15 M NaCl solution at 25 °C. The dimensions used (*see* Table 2) are those obtained from light and electron micrographs of gallbladders fixed in the absence and presence of osmotic gradients. The equivalent circuits for the two alternative pathways across the epithelium and the equivalent circuit, which takes into account the role of the submucosa, are shown in Fig. 12*a*, *b* and *c*, respectively.

Preliminary calculations of this type showed that in the absence of water flow across the gallbladder: (a) the combined intercellular spaces of the epithelium, the submucosa and the muscularis, contribute less than 4% of the total electrical resistance of the tissue. This is consistent with previous experimental observations which showed that the epithelium accounted for more than 94% of the gallbladder resistance (Wright & Diamond, 1968); (b) the lateral intercellular spaces do not offer a significant diffusion barrier to the movement of sucrose and 1,4-butanediol across the gallbladder; and

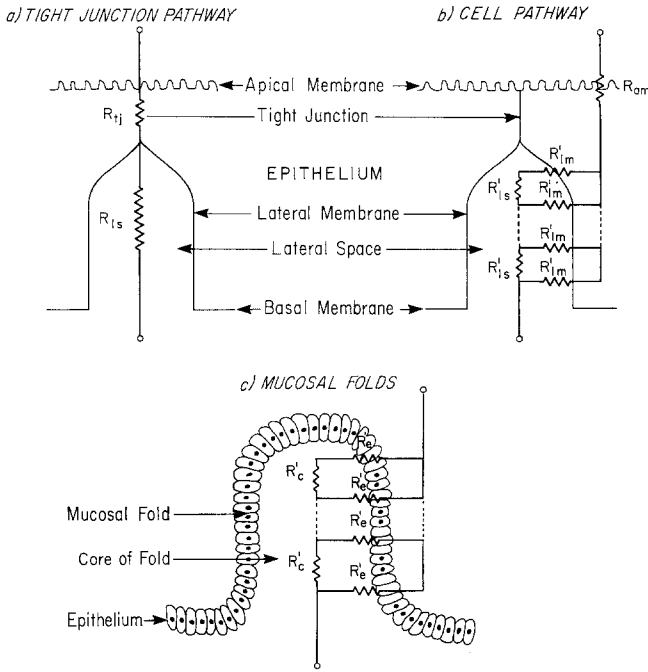


Fig. 12. Equivalent circuit diagrams for permeation across the gallbladder epithelium and mucosal folds. (a) Permeation via the tight junction pathway: R_{tj} is the resistance of the tight junctions (electrical or diffusional) and R_{ls} is the resistance of the lateral spaces. The permeability coefficient for the epithelium, P_e , is given by $1/P_e = 1/P_{tj} + 1/P_{ls}$, and P_{ls} is given by $D A/l$, where D is the free solution diffusion coefficient, A the area of the space and l the length of the space. (b) Permeation via the cellular pathway: R_{am} , R'_{lm} and R'_{ls} are the resistances of the apical cell membrane, lateral cell membrane and lateral space, respectively. It is assumed that the resistance of the cytoplasm is negligible compared with R_{am} , R'_{lm} and R'_{ls} . In this case the P_e is given by $1/P_e = 1/P_{am} + 1/P_{lm/ls}$ where $P_{lm/ls}$ is the permeability coefficient for the lateral membrane/lateral space network. The permeability of the network is given by the expression

$$P_{lm/ls} = \frac{1}{\sqrt{\frac{1}{P'_{ls}} \times \frac{1}{P'_{lm}} \coth \sqrt{\frac{P'_{lm}}{P'_{ls}} l}}}$$

if it is assumed that it can be represented by a distributed network terminated in an open circuit (see LePage & Seely, 1952, Eq. 9.76), i.e., there is a negligible flux across the basal cell membrane. This is a reasonable approximation since the area of the lateral membrane is much greater than the area of the basal membrane. $P'_{lm}(1/R'_{lm})$ is the permeability of the lateral cell membrane, $P'_{ls}(1/R'_{ls})$ is the permeability of the lateral space (both expressed per unit length of the lateral space) and l is the length of the space. (c) Permeation across the mucosal folds: The circuit diagram is analogous to that in (b) except that R'_e and R'_c are the resistances of the epithelium and core of the fold expressed per unit length of the fold. In the absence of water flows and with osmotic water flows directed towards the mucosal fluid only 50% of the epithelial cells are on the mucosal folds. For further details see the text

(c) the sub-epithelial tissues constitute the serosal unstirred layer which provides a "barrier" to the passage of highly permeant solutes across the gallbladder (*see Smulders & Wright, 1971*). It follows that when water is flowing towards the serosa, the lateral intercellular spaces, the submucosa and muscularis form even less of a diffusion barrier because the extracellular spaces dilate widely under these conditions (*see Figs. 6a and 7a*). This is verified by computations which predict, and experiments which show, that there is no increase in the permeability of the gallbladder upon addition of sucrose to the serosal solution (e.g., *see Figs. 2 and 4*).

On the other hand, calculations do predict a significant reduction in the permeability of the gallbladder when sucrose is added to the mucosal fluid. In Table 3 we show the changes in G , P_{sucrose} and $P_{1,4\text{-butanediol}}$ predicted from the changes in tissue geometry. Also included, for comparison, are the permeability changes actually observed. To illustrate the procedure used to compute these permeability coefficients we have included the following calculation:

Let us predict the change in P_{sucrose} when 300 mM sucrose is added to the mucosal solution. It is assumed that the major pathway for sucrose permeation across the epithelium is the tight junction route (Fig. 12a). The first step is to calculate the permeability coefficient for the tight junction (P_{tj}). This is obtained from the relationship

$$1/P_{tj} = 1/P_e - 1/P_{ls} \quad (1)$$

where P_e and P_{ls} are the permeability coefficients for the epithelial layer and the lateral spaces, respectively. In the absence of osmotic flow across the gallbladder $P_{\text{sucrose}} = 2.7 \times 10^{-6}$ cm/sec (Table 3) and this is considered to be the permeability coefficient for the epithelium (Smulders & Wright, 1971). The permeability of the lateral spaces is given by the expression

$$P_{ls} = DA/l \quad (2)$$

where A and l are the area and length of the lateral spaces, respectively, and D is the sucrose diffusion coefficient. In the absence of flow $P_{ls} = 2.08 \times 10^{-4}$ cm/sec ($D = 5.2 \times 10^{-6}$ cm²/sec, $A = 0.12$ cm²/cm² and $l = 30 \times 10^{-4}$ cm). Substitution of P_{ls} and P_e into Eq. (1) shows that $P_{tj} = 2.73 \times 10^{-6}$ cm/sec. Since $P_{ls} \gg P_{tj}$ it follows that the permeability of the epithelium to sucrose is controlled by the tight junctions in the absence of water flow.

In the presence of 300 mM sucrose in the mucosal fluid there is a decrease in the dimensions of the lateral spaces which suggests a decrease in P_{ls} . Substitution of the dimensions ($A = 0.01$ cm²/cm², $l = 60 \times 10^{-4}$ cm) into Eq. (2) shows that P_{ls} is reduced to 8.67×10^{-6} cm/sec, and substitution of this, in turn, into Eq. (1) predicts that the permeability of the epithelium is reduced to 2.08×10^{-6} cm/sec. Comparison of this coefficient with the permeability coefficient actually observed (Table 3) shows that the change in dimensions of the lateral spaces accounts for about 30% of the change in sucrose permeability.

Although the submucosal tissue is not a barrier to the movement of sucrose across the gallbladder in the absence of osmotic flow, it is possible that the collapsed mucosal folds observed in the presence of osmotic flow towards the mucosa (Fig. 7c) are a signifi-

cant barrier. The equivalent circuit used to determine the permeability of the collapsed folds is shown in Fig. 12*c*. The permeability of the folds (P_f) is given by the expression

$$P_f = \frac{1}{\sqrt{\frac{1}{P'_c} \times \frac{1}{P'_e} \coth \sqrt{\frac{P'_e}{P'_c}} l}} \quad (3)$$

where $P'_e (\equiv P_e^*/l)$ is the permeability of the epithelium per unit length of fold, $P'_c (\equiv P_c/l)$ is the permeability of the core of the fold per unit length, and l is the length of the fold. This expression is similar in form to that derived for the input impedance in a distributed network with open circuit termination (*see* Lepage & Seely, 1952, Eq. 9.76). $P_c = DA/l = 1.16 \times 10^{-6}$ cm/sec and $P_e^* = P_e/2 = 1.04 \times 10^{-6}$ cm/sec ($l = 90 \times 10^{-4}$ cm, $A = 2 \times 10^{-4}$ cm²/cm², $D = 5.2 \times 10^{-6}$ cm²/sec and $P_e = 2.08 \times 10^{-6}$ cm/sec; we divide P_e by 2 since only 50% of the cells are on the folds). Substitution of these parameters into Eq. (3) and adding P_f (8×10^{-7} cm/sec) to the permeability coefficient for the cells not on the folds (1.0×10^{-6} cm/sec) yields a sucrose permeability coefficient of 1.8×10^{-6} cm/sec. Comparison of this with the coefficient obtained experimentally (Table 3) shows that the collapse of the folds accounts for only about 10% of the observed change in permeability.

The results in Table 3 show that we can expect changes in the permeability of the gallbladder from the changes in geometry of the tissue alone. In general, the reduction in the permeability to both ions and nonelectrolytes is between 30 and 80% of the permeability changes actually observed. As

Table 3. The effect of osmotic gradients on the permeability of the gallbladder; experimental and theoretical

Osmotic gradient (mosm)	Conductance (mmho)		P_{sucrose} (cm/sec $\times 10^6$)		$P_{1,4\text{-butanediol}}$ (cm/sec $\times 10^5$)	
$\Delta\pi = 0$	24		2.7		2.3	
	pred.	obs.	pred.	obs.	pred.	obs.
$\Delta\pi = 50$	17	14	2.4	2.0	1.7	1.5
$\Delta\pi = 300$	10	7	1.8	0.6	1.1	0.7

Shown are the electrical conductance, P_{sucrose} and $P_{1,4\text{-butanediol}}$ in the presence and absence of sucrose (50 and 300 mM) in the mucosal fluid. At the two osmotic gradients both the observed and the predicted permeability coefficients are shown. Parameters are predicted from the changes in tissue geometry (Table 2) assuming that sucrose and current cross the epithelium via the tight junction route (Fig. 12*a*) and that 1,4-butanediol permeates via the cellular route (Fig. 12*b*). In the latter case it was assumed that the area of the lateral membranes was ten times greater than the area of the apical membrane and that the permeability coefficients for the two membranes were identical. All parameters are expressed in terms of the epithelial surface area which is 1.5 times greater than the serosal surface area. The conductance values were obtained in six experiments whereas the permeability coefficients were obtained in at least two gallbladders. The permeability coefficients in each experiment were normalized to the average values obtained in the absence of osmotic gradients by Smulders and Wright (1971). For further details *see* Fig. 12 and the text.

seen in the sample calculation, the most important change in structure is the collapse of the lateral intercellular spaces, which, in general, accounts for about three-fourths of the computed decrease in permeability. It should be noted that the changes in tissue geometry account for the changes in permeability equally well at the two osmotic gradients.

It is readily apparent from the equivalent circuit diagrams (Fig. 12*a, b*) that the collapse of the lateral channels should produce the greatest effect on those solutes that permeate via the tight junctions. Thus, the computed values for P_{sucrose} and G , calculated for the tight junction pathway, represent the maximum effect. On the other hand, $P_{1,4\text{-butanediol}}$ calculated for the cellular pathway, would be too high (by a factor of 1.5) if this solute also follows the tight junction route. In principle, it is possible to decide which pathway 1,4-butanediol uses to cross the epithelium by comparing the predicted permeability coefficients for the two pathways with the experimental values. Unfortunately, because of the assumptions and uncertainties involved in these calculations (*see* below) and the low magnitude of the difference between the predicted permeability coefficients, we cannot definitely conclude that 1,4-butanediol follows the cellular route. Perhaps this question will be resolved by autoradiographic techniques.

Sources of Uncertainty

Three sources of uncertainty surround our attempt to quantitatively relate structure to permeability. The first concerns the general problem of how much chemical fixation and subsequent tissue processing alters the dimension of the tissue. For example, direct light microscopy of cells (Borysko, 1964) and of isolated renal proximal tubules (Grantham & Tormey, *unpublished*) suggests that cellular shrinkage invariably accompanies dehydration and embedding for electron microscopy. The second concerns the assumption that the properties of the solution in the collapsed lateral spaces are identical to those of a bulk phase solution. These might be modified by membrane surface charges, extraneous membrane coats, and the narrow dimensions of the space (*cf.*, Schultz & Asunmaa, 1970; Bean, 1971, for discussion of some of these effects). The restriction of diffusion in the lateral spaces by the proximity of the lateral membranes may be estimated from the equation

$$D'/D = \frac{(1-r/w)}{1+3.4(r/w)^2} \quad (4)$$

(Pappenheimer, Renkin & Borrero, 1951) where D' and D are the solute diffusion coefficients in the channel and free solution, respectively, r the

radius of the solute, and w half the distance between the lateral membranes. [The validity of this type of equation has recently been verified for 50 Å channels in mica membranes (Beck & Schultz, 1970).] For sucrose ($r = 5$ Å) the diffusion coefficient is reduced by about 10% when the lateral spaces are collapsed (i.e., 100 Å wide). Therefore, the physical proximity of the lateral membranes *per se* does not produce a significant reduction in the diffusion coefficients in the channel. However, mucosubstances, which are widely believed to form extraneous coats on the surfaces of plasma membranes, might limit diffusion in narrow channels by virtue of both their electrical and mechanical properties. Although many of our electron images suggest the presence of a "fuzzy" material on the lateral membranes, we are reluctant to draw any conclusion on this basis. PAS staining of the lateral membranes has also been negative in our hands (Tormey & Diamond, 1967). However, some histochemical studies suggest that the absence of fuzzy material and of PAS staining do not rule out the presence of surface coats (e.g., Pease, 1966). If the properties of the solution in the collapsed lateral spaces are not identical to those of a bulk phase solution this would mean that in our calculations we are underestimating the change in permeability. Finally, because of these uncertainties we have used simplifying assumptions to extract the parameters listed in Table 2 rather than analyzing the electron microscopic data more rigorously. More precise dimensions could have been obtained by the application of quantitative stereology to the analysis of a large number of micrographs, but the gain in rigor would be illusory because of the other uncertainties.

Nevertheless, in spite of these uncertainties we conclude that osmotically induced permeability changes in the rabbit gallbladder are largely accounted for by the change in tissue geometry, the dominant effect being the collapse of the lateral intercellular spaces.

Additional Lines of Evidence

There are three other lines of evidence which support our hypothesis that osmotically induced changes in gallbladder permeability are due to the collapse of the lateral spaces.

(1) *The Transport Number Effect.* The polarization potentials which appear in the presence of osmotic water flows (*see* p. 174) are probably due to the transport number effect (*see* Barry & Hope, 1969*a, b*; Wedner & Diamond, 1969). Both the polarity and the time course of the polarization potentials observed are qualitatively very similar to those observed at much higher current densities (1 to 6 mamp) in the gallbladder in the absence of

osmotic gradients (Wedner & Diamond, 1969). The polarization potentials indicate current-induced changes in the salt concentration in the solution adjacent to the serosal face of the epithelial cells. The magnitude of the changes in salt concentration depends upon: (a) the ion transport numbers in both the gallbladder membranes and in the serosal unstirred layers; (b) the thickness of the serosal unstirred layer; and (c) the current density. In the presence of osmotic flows from the serosal to the mucosal solutions there is an actual reduction in the thickness of the serosal unstirred layer (*see Paper 2*) and there is no apparent change in the transport numbers (*unpublished observations*). The appearance of the transport number effect must then be due to an effective increase in the current density in the lateral channels since osmotic flow towards the mucosal solution reduces the width of the lateral channels.

(2) *Current-Induced Resistance Changes*. Associated with the appearance of the polarization potentials are the current-induced changes in gallbladder resistance. These resistance changes are similar, but smaller, to those observed by Frömter (*personal communication*) in the *Necturus* gallbladder. They are probably related to the electrically-induced changes in the widths of the lateral spaces observed by Frömter (*personal communication*) in the *Necturus* gallbladder and by Gfeller, Ferris and Walser (1971) in the toad urinary bladder. The change in width of the lateral spaces could, in turn, be related to water flows associated with the transport number effect (*see Barry & Hope, 1969a, b, and Wedner & Diamond, 1969, for a detailed discussion of current-induced water flows*). When a current is passed across the gallbladder such that the mucosal solution goes negative, there is water flow from the serosal to the mucosal solutions (Wedner & Diamond, 1969) and this, according to Fig. 3, should cause an increase in gallbladder resistance. In fact, we did observe an increase in the resistance when current was passed in this direction (*see p. 174*) but only when the spaces were partially closed by addition of sucrose to the mucosal fluid, i. e., the changes in resistance brought about by current flow are only apparent when the resistance of the lateral spaces approaches the resistance of the tight junctions.

(3) *Changes in the Ratio of the Apical Membrane Resistance to the Lateral-Basal Membrane Resistance*. The relative resistance of the apical cell membrane to the lateral-basal cell membrane was measured by Frömter (*personal communication*) who passed a current across *Necturus* gallbladder and measured the voltage drops across the two cell membranes. The ratio of the apical membrane resistance to the lateral-basal membrane resistance was about 2, but when sucrose (600 mM) was added to the mucosal solution

this ratio dropped to about 0.2. Associated with the changes in cell membrane resistance was a twofold increase in the transepithelial resistance (*cf.* Fig. 3). The increase in the effective resistance of the lateral-basal membrane must be related, at least in part, to the collapse of the lateral spaces and the concomitant increase in the resistance of these spaces.

The Mechanism of the Structural Changes

Having established that alterations in the geometry of the lateral intercellular spaces are the major explanation for the physiological observations, we are still left with the question of why this geometry changes. Under resting conditions the intercellular spaces are slightly open and even when the spaces have been closed by osmotic gradients they readily reopen when the osmotic gradients are removed. In the absence of demonstrable changes in cell volume, it seems likely that further opening of the spaces requires a positive pressure within the space and closure requires a negative pressure.

The development of such pressures necessitates the existence of one or more hydraulic barriers between the open end of the spaces and the serosal surface of the tissue. Our results clearly show the subserosal layer to be a significant barrier. Water flow directed towards the serosa forced the muscle cells apart and enormously increased the volumes of both the submucosa and the muscularis. Water flow towards the mucosa produces exactly the reverse effect. The subserosa is the only potential barrier appropriately situated to alter the hydrostatic pressure within these layers and produce these effects. Nevertheless, several other potential barriers are also present. For example, the basement membrane of the epithelium must be seriously considered, especially since Grantham (*personal communication*) has recently demonstrated that the basement membranes of renal tubules have an appreciable hydraulic resistance. The muscularis itself may also be a significant barrier. At present we have no basis for evaluating the relative significance of the subserosa, muscularis and basement membranes as hydraulic barriers.

The location of the hydraulic barrier or barriers in the sub-epithelial tissues has implications regarding the mechanism of alterations in the dimensions of the lateral channels. *A priori* these channels might dilate or collapse because the hydraulic resistance of the basement membrane is sufficiently high to produce pressure changes within the channels. Alternatively, if the hydraulic resistance of the basement membrane were too small, pressures sufficient to alter lateral space geometry might be generated in the submucosa. In the latter case one could not conclude whether altered space dimensions were the results of flow through the lateral spaces or not.

However, there is some evidence to suggest that pressures within the submucosa are inadequate to produce dilation of the lateral spaces, namely, unphysiologically high pressures are required on the serosal surface of the gallbladder to dilate the spaces (Tormey & Diamond, 1967). But whatever the actual mechanism by which water flows alter intercellular space dimensions in the epithelium, the evidence presented in the following paper strongly suggests that the major route for water flow across the gallbladder epithelium is via the lateral intercellular spaces.

Conclusions

We have shown that the osmotically induced changes in the permeability of the rabbit gallbladder to ions and nonelectrolytes are largely accounted for by the changes in the dimensions of the lateral intercellular spaces. It therefore follows that the lateral spaces are the major pathway by which a wide variety of solutes cross the epithelium. This is a common pathway for solutes which permeate across the epithelium via the tight junction route and for solutes which permeate through the epithelial cells. Although it is not altogether clear how osmotic water flows change the dimensions of the lateral spaces, our interpretation about the route of solute transport is completely independent of this question. Finally, preliminary observations suggest that these conclusions also apply to other epithelial membranes such as the intestine, renal tubule and choroid plexus. Thus, great care must be exercised in the interpretation of transport parameters in these membranes to ensure that the conclusions drawn are independent of structural changes within the tissue.

We wish to thank Drs. P. H. Barry, J. M. Diamond, R. E. Eisenberg, J. Leung and W. New for helpful suggestions and advice during the course of this study, Dr. E. Frömter for permission to cite unpublished results, and Drs. J. M. Diamond, R. E. Eisenberg and E. Frömter for their critical review of the manuscript. The project was supported by grants from the Life Insurance Medical Research Fund (G-69-19) and the United States Public Health Service (AM-12621 and HE-03067). Phyllis Lee and Pat Ilg provided technical assistance and one of the authors (A.P.S.) was a predoctoral fellow under USPHS training grant GM-00448.

References

- Barry, P. H., Diamond, J. M. 1970. Junction potentials, electrode standard potentials, and other problems in interpreting electrical properties of membranes. *J. Membrane Biol.* 3:93.

- Barry, P. H., Diamond, J. M., Wright, E. M. 1971. The mechanism of cation permeation in rabbit gallbladder: Dilution potentials and biionic potentials. *J. Membrane Biol.* **4**:358.
- Barry, P. H., Hope, A. B. 1969*a*. Electro-osmosis in membranes: Effects of unstirred layers and transport numbers. Pt. I. Theory. *Biophys. J.* **9**:700.
- Barry, P. H., Hope, A. B. 1969*b*. Electro-osmosis in membranes: Effects of unstirred layers and transport numbers. Pt. II. *Exp. Biophys. J.* **9**:729.
- Bean, C. P. 1971. The physics of porous membranes. In: Membranes, A Series of Advances, Vol. 1. G. Eisenman, editor. p. 1. Marcel Dekker Inc., New York.
- Beck, R. E., Schultz, J. S. 1970. Hindered diffusion in microporous membranes with known pore geometry. *Science* **170**:1302.
- Bentzel, C. J., Parsa, B., Hare, D. K. 1969. Osmotic flow across the proximal tubule of *Necturus*. Correlation of physiologic and anatomic studies. *Amer. J. Physiol.* **217**:570.
- Berridge, M. J., Gupta, B. L. 1967. Fine-structural changes in relation to ion and water transport in the rectal papillae of the blowfly, *Calliphora*. *J. Cell Sci.* **22**:89.
- Borysko, E. 1956. Recent developments in methacrylate embedding. I. A study of the polymerization damage phenomenon by phase contrast microscopy. *J. Biophys. Biochem. Cytol.* **2**:3 (supplement).
- Dainty, J. 1963. Water relations of plant cells. *Advanc. Bot. Res.* **1**:279.
- Diamond, J. M. 1962. The mechanism of solute transport by the gallbladder. *J. Physiol.* **161**:474.
- Diamond, J. M., Bossert, W. H. 1967. Standing-gradient osmotic flow: A mechanism for coupling of water and solute transport in epithelia. *J. Gen. Physiol.* **50**:2071.
- Diamond, J. M., Tormey, J. McD. 1966. Role of long extra-cellular channels in fluid transport across epithelia. *Nature* **210**:817.
- Frömter, E., Diamond, J. M. 1972. The route of passive ion permeation in epithelia. *Nature* **235**:9.
- Frömter, E., Lüer, K. 1969. Determination of fixed-charge concentration in the epithelium of the convoluted tubule of the rat kidney. The effect of pH. *Pflüg. Arch. Ges. Physiol.* **307**:R 76.
- Gfeller, E., Ferris, F., Walser, M. 1971. The effect of electrically induced changes in Na transport on width of lateral spaces in toad bladder epithelium. *Fed. Proc.* **30**:421 (Abs).
- Grantham, J., Cuppage, F. E., Fanestil, D. 1971. Direct observation of toad bladder response to vasopressin. *J. Cell Biol.* **48**:695.
- Grantham, J. J., Ganote, C. E., Burg, M. B., Orloff, J. 1969. Paths of transtubular water flow in isolated renal collecting tubules. *J. Cell Biol.* **41**:562.
- Kaye, G. I., Wheeler, H. O., Whitlock, R. T., Lane, N. 1966. Fluid transport in the rabbit gallbladder: a combined physiological and electron microscopic study. *J. Cell. Biol.* **30**:237.
- LePage, W. R., Seely, S. 1952. General Network Analysis. McGraw-Hill Book Co., Inc., New York.
- Loeschke, K., Bentzel, C. J., Csáky, T. Z. 1970. Asymmetry of osmotic flow in frog intestine: functional and structural correlation. *Amer. J. Physiol.* **218**:1723.
- Pappenheimer, J. R., Renkin, E. M., Borrero, L. M. 1951. Filtration, diffusion and molecular sieving through peripheral capillary membranes: A contribution to the pore theory of capillary permeability. *Amer. J. Physiol.* **167**:13.
- Pease, D. C. 1966. Polysaccharides associated with the exterior surface of epithelial cells: Kidney, intestine, brain. *J. Ultrastruct. Res.* **15**:555.
- Schultz, R. D., Asunmaa, S. K. 1970. Ordered water and the ultrastructure of the cellular plasma membrane. In: Recent Progress in Surface Science, Vol. 3, p. 291.

- J. F. Danielli, A. C. Riddiford and M. D. Rosenberg, editors. Academic Press Inc., New York.
- Smulders, A. P., Wright, E. M. 1971. The magnitude of nonelectrolyte selectivity in the gallbladder epithelium. *J. Membrane Biol.* **5**:297.
- Tormey, J. McD. 1964. Differences in membrane configuration between osmium tetroxide-fixed and glutaraldehyde-fixed ciliary epithelium. *J. Cell Biol.* **23**:658.
- Tormey, J. McD., Diamond, J. M. 1967. The ultrastructural route of fluid transport in rabbit gallbladder. *J. Gen. Physiol.* **50**:2031.
- Tormey, J. McD., Smulders, A. P., Wright, E. M. 1971. A common pathway for active and passive water and solute fluxes across gallbladder epithelium. *Fed. Proc.* **30**:422 (Abs.).
- Tormey, J. McD., Wright, E. M., Smulders, A. P. 1971. Tracing permeation pathways across epithelia. *Proc. 29th Ann. Meeting Electron Microscope Soc. Amer.* p. 394.
- Wedner, H. J., Diamond, J. M. 1969. Contributions of unstirred-layer effects to apparent electrokinetic phenomena in the gallbladder. *J. Membrane Biol.* **1**:92.
- Wright, E. M., Barry, P. H., Diamond, J. M. 1971. The mechanism of cation permeation in rabbit gallbladder: Conductances, the current-voltage relation, the concentration dependence of anion-cation discrimination, and the calcium competition effect. *J. Membrane Biol.* **4**:331.
- Wright, E. M., Diamond, J. M. 1968. Effects of pH and polyvalent cations on the selective permeability of gall bladder epithelium to monovalent ions. *Biochim. Biophys. Acta* **163**:57.
- Wright, E. M., Diamond, J. M. 1969a. An electrical method of measuring non-electrolyte permeability. *Proc. Roy. Soc. (Lond.) B* **172**:203.
- Wright, E. M., Diamond, J. M. 1969b. Patterns of non-electrolyte permeability. *Proc. Roy. Soc. (Lond.) B* **172**:227.
- Wright, E. M., Smulders, A. P., Tormey, J. McD. 1972. The role of the lateral intercellular spaces and solute polarization effects in the passive flow of water across the rabbit gallbladder. *J. Membrane Biol.* **7**:198.